



Large and spatial magnetic field modulation using superconducting bulk magnet and silicon steel

H. Fujishiro*, D. Furuta, K. Yaegashi, T. Naito, N. Yoshimoto

Faculty of Engineering, Iwate University, 4-3-5 Ueda, Morioka 020-8551, Japan

ARTICLE INFO

Article history:
Available online 16 May 2010

Keywords:
Magnetic modulation
Magnetic force
Superconducting bulk magnet
Magnetic circuit
The Moses effect

ABSTRACT

As an application of superconducting bulk magnets to a solution growth of organic semiconductor films by means of “the Moses effect”, we have investigated the realization of the spatially modulated magnetic field using two-aligned superconducting bulk magnets and silicon steel bundles. Two bulks were magnetized by pulsed fields with an opposite magnetic polarity of over 2 T and were magnetically coupled with the three pairs of the ferromagnetic bundles stacked by thin silicon steel sheets with a narrow open gap. To maximize the magnetic force in the gap, we measured systematically the spatial magnetic field modulation ΔB and the magnetic force coefficient BdB/dx , as functions of the thickness of the bundles (W), the space between the bundles (S) and the open gap width (G). As a result, $\Delta B = 0.76$ T and $BdB/dx = 500$ T²/m were realized in the gap under the conditions of $W = 1.4$ mm, $S = 6$ mm and $G = 1$ mm.

© 2010 Elsevier B.V. All rights reserved.

1. Introduction

Recently, electronic devices using organic semiconductors such as pentacene and oligothiophenes have been widely developed because of a low-cost and low-temperature fabrication process on large and flexible substrates [1–3]. However, in general, the electron mobility μ_e in organic semiconductors is fairly smaller than that of crystalline silicon and other inorganic semiconductors because of large amount of crystal defects and a misalignment of the crystallites. A solution growth of organic semiconductors is a promising technique for the practical applications because of the growth under a quasi-equilibrium condition. To realize the high μ_e in the grown film, it is necessary to grow the large crystallites and to align the crystal axes by some techniques. We have so far investigated the crystal growth of organic semiconductors from solution phase [4], and have applied magnetic field higher than 2 T to the solution by using a superconducting bulk magnet. The thickness of the diamagnetic solvent such as tetra-hydrofuran (THF) became very thin by means of “the Moses effect” [5] and the single-crystalline film of organic semiconductor started to grow preferentially from the edge of the thin solution layer because of a supersaturation. As a result, the grown thin film can be highly oriented along the magnetic gradient [6]. If the solution growth is performed under a deep and spatially minute magnetic field on the substrate, the highly oriented growth pattern of the organic semiconductor can be fabricated by “the micro-Moses effect” [7] without any photolithography processes, which reproduces the magnetic pattern.

In this paper, we have investigated the realization of spatially modulated magnetic field. Two-aligned superconducting bulk magnets higher than 2 T, which had the usable surface on both sides in open space, were magnetically coupled with the ferromagnetic bundles of silicon steel sheets with a narrow open gap. To maximize the spatial magnetic field modulation in the gap, we measured the magnetic field profiles, as functions of the thickness of the bundles (W), the space between the bundles (S), and the open gap width (G).

2. Experimental procedure

Fig. 1 shows the schematic view of the experimental setup and the dimension of the apparatus. Highly *c*-axis oriented SmBaCuO and YBaCuO bulk disks (Dowa Mining Corp.) 45 mm in diameter and 15 mm in thickness were tightly fastened with the brass bar from the side face and the bar was attached to the cold stage of a Gifford McMahon (GM) cycle helium refrigerator. The distance between the bulk centers was 60 mm. The bulks were cooled to 40 K in a vacuum sheath and the pulse fields of $B_{ex} = 5.5$ T were applied twice for each bulk using the split-type pulse coil dipped in liquid N₂. The polarity of the applied pulse fields was opposite for each bulk, and the maximum trapped fields were +2.36 T and –1.80 T at the top surface of the vacuum sheath just on the SmBaCuO and YBaCuO bulk disk, respectively. Nearly the same magnitude of the trapped field was observed on the rear surface of the vacuum sheath with an opposite polarity. The detailed magnetizing process is described elsewhere [8].

Two bulk magnets were magnetically coupled with the three paths of grain-oriented silicon (electrical) steel bundles with a narrow open gap. The silicon steel sheets (JFE Steel Corp.) with

* Corresponding author. Tel./fax: +81 19 621 6363.
E-mail address: fujishiro@iwate-u.ac.jp (H. Fujishiro).

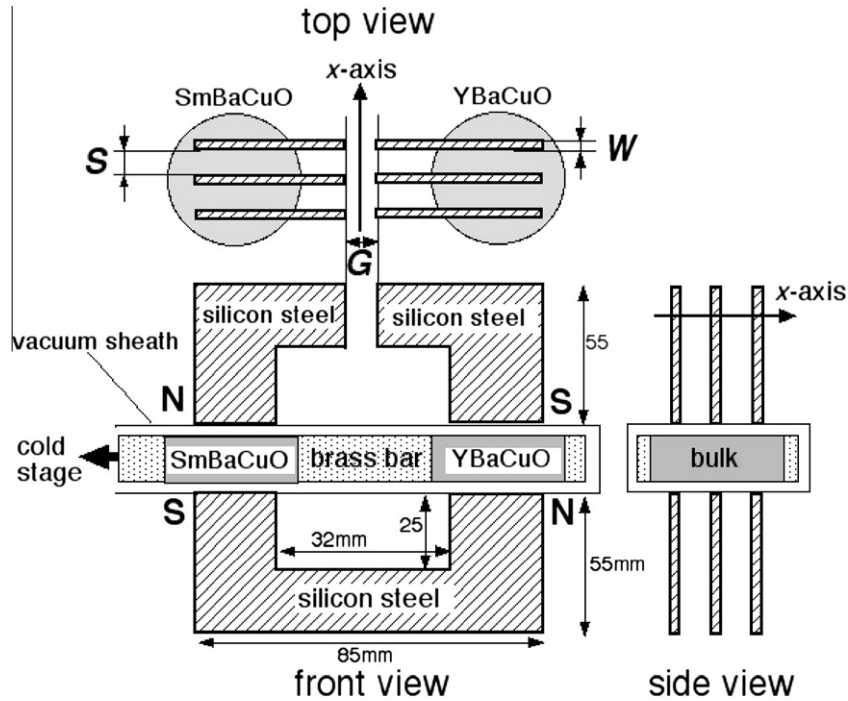


Fig. 1. The experimental setup and the dimensions of the apparatus used in this study.

0.35 mm in thickness were stacked up to four sheets and the thickness of the bundles (W) was changed from 0.35 mm to 1.4 mm. The permeability μ_m and the saturation moment B_s are 5.3×10^4 and 2.03 T, respectively. The bundles were separated using spacers made by acrylic plates and the space between the bundles (S) was changed from 3 mm to 9 mm. The width of the open gap (G) was changed from 1 mm to 6 mm. The spatial magnetic modulation in the gap was measured as functions of the W , S and G values using a Tesla meter (F.W. BELL 5080).

3. Results and discussion

Fig. 2 shows the x dependence of the magnetic field $B(x)$ in the gap for various thicknesses of the bundles W under the conditions of $G = 2$ mm and $S = 6$ mm. The magnetic field modulation changes depending on the W value. Hereafter, we define the magnitude of the magnetic field modulation ΔB as the difference between the

maximum magnetic field B_{max} at the central bundle and the local minimum magnetic field B_{min} in the neighbor ($\Delta B = B_{max} - B_{min}$). For smaller W value, the B_{max} value was small because of the small cross section of the silicon steel bundles and, therefore, the ΔB value was also small. On the other hand, the ΔB value increases concomitantly with increasing W . The trapped field profile of the SmBaCuO bulk on the vacuum sheath is also shown in the right axis of ordinates in Fig. 2 as a dotted line. The maximum trapped field was 2.36 T. The shape of $B(x)$ was conical and $B(x)$ decreased with increasing distance from the bulk center. The trapped field profile of the YBaCuO bulk on the vacuum sheath was also a conical shape.

Fig. 3 shows the x dependence of the magnetic field $B(x)$ in the gap for various S values under the conditions of $W = 1.4$ mm and $G = 2$ mm. The B_{max} value was independent of the S value. However, the B_{min} value decreases concomitantly with increasing S . Because the measured $B(x)$ in the gap was overlapped by the magnetic field contributed from the neighbor bundles. As a result,

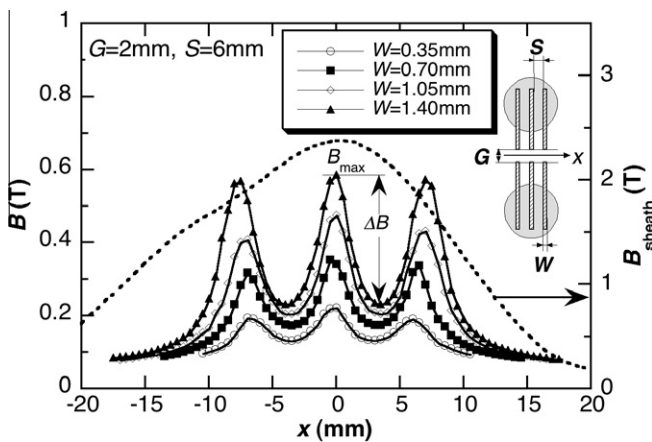


Fig. 2. The x dependence of the magnetic field $B(x)$ in the gap for various thicknesses of the silicon steel bundles W under the conditions of $G = 2$ mm, $S = 6$ mm.

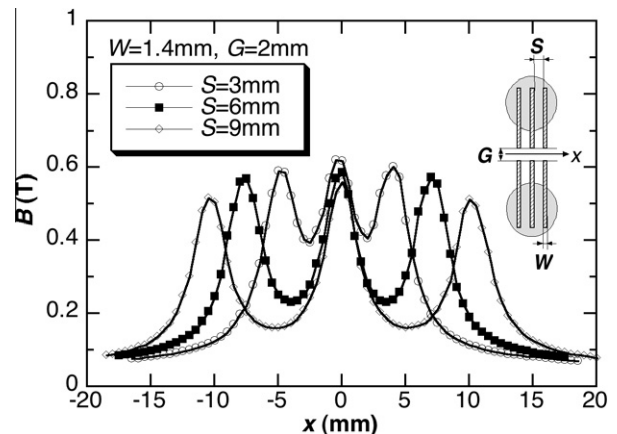


Fig. 3. The x dependence of the magnetic field $B(x)$ in the gap for various spaces between bundles S under the conditions of $W = 1.4$ mm and $G = 2$ mm.

the overlap was enhanced and the ΔB value decreased with decreasing S . It is noteworthy that the magnitude of maximum B value on the outer bundles was lower than B_{\max} on the central bundle because of the conical B profile of the bulk superconducting bulks as shown in Fig. 2.

Fig. 4 shows the x dependence of the magnetic field $B(x)$ in the gap for various widths of the open gap G under the conditions of $W = 1.4$ mm and $S = 6$ mm. For a large G value, the magnetic connection becomes weak because of the leakage flux in the magnetic circuit. As a result, ΔB and B_{\max} were small. With decreasing G value, ΔB increased sensitively. The maximum ΔB value of 0.76 T was obtained in this study by the condition of $G = 1$ mm.

As mentioned above, the ΔB and B_{\max} values change depending on the values of G , W and S . Figs. 5a and 5b summarizes the ΔB values as functions of W and S values for each G value. The ΔB value increases with increasing W and also increases with increasing S . Furthermore, the ΔB increases sensitively with decreasing G . To enhance the magnetic modulation more and more, the W and S values might be increased. However, the enhancement of ΔB is restricted because of the finite diameter of the bulk magnets. The B_{\max} value ought to be increased up to the saturation magnetization of the used silicon steel ($=2.03$ T).

Fig. 6 shows the analyses of the measured magnetic field modulation profile for the conditions of $W = 1.05$ mm, $S = 6$ mm and $G = 2$ mm. In the figure, closed circles show the measured modulation. The dotted line depicts the estimated background magnetic

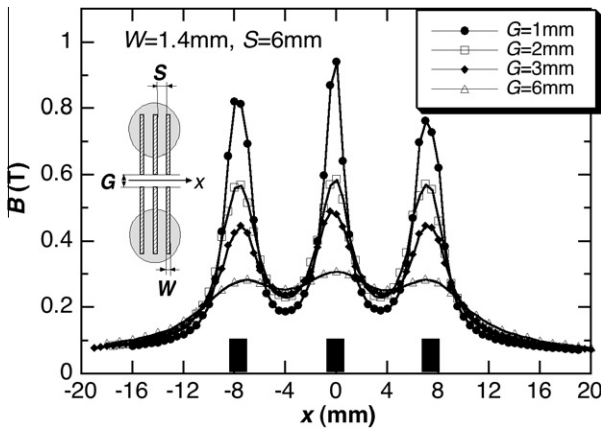


Fig. 4. The x dependence of the magnetic field $B(x)$ in the gap for various widths of the open gap G under the conditions of $W = 1.4$ mm and $S = 6$ mm.

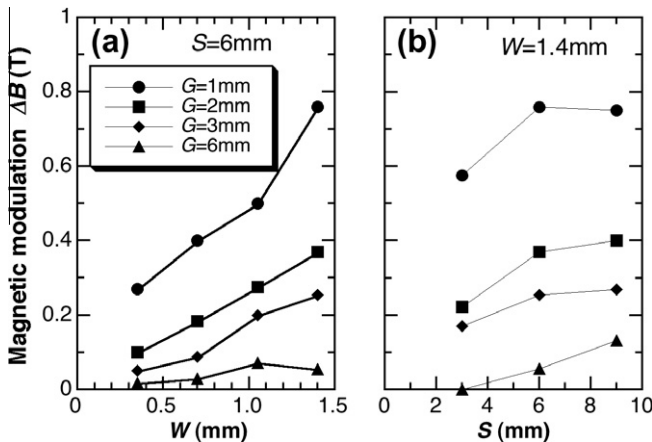


Fig. 5. The magnitude of the magnetic modulation ΔB , as functions of W and S values for each G value.

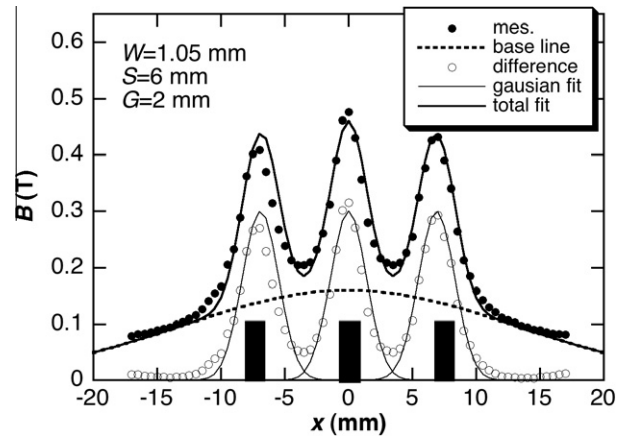


Fig. 6. The analyses of the measured magnetic field modulation for the conditions of $W = 1.05$ mm, $S = 6$ mm and $G = 2$ mm (see text).

field profile using a Gaussian function, which results from the leakage flux passing through the spaces between the silicon steel bundles. The open circles show the contribution from the silicon steel bundles, which are subtracted for the estimated background profile from the measured ones. The thin solid lines are the Gaussian fits for the contribution from the each bundle. The measured profile can be reproduced by the contributions of both concentrated flux to the bundles and the leakage flux as shown in the thick bold line.

Figs. 7a and 7b show the magnetic gradient dB/dx and the magnetic force coefficient BdB/dx profiles for the condition ($W = 1.4$ mm, $S = 6$ mm, $G = 1$ mm), at which ΔB was the largest in this study. For comparison, those for the condition ($W = 1.4$ mm, $S = 6$ mm, $G = 2$ mm) and those on the vacuum sheath were also shown. The magnetic force F_M is proportional to the magnetic force coefficient BdB/dx ; not only the magnetic field B , but also magnetic field gradient ($\text{grad } B$) generated on the bulk. The maximum values ($dB/dx = 600$ T/m, $BdB/dx = 500$ T²/m) for $G = 1$ mm are higher than those on the vacuum sheath. These specific values are about 10 times as large as those for the Nd-Fe-B permanent magnet and are important parameters for the Moses effect. These values were drastically suppressed for $G = 2$ mm.

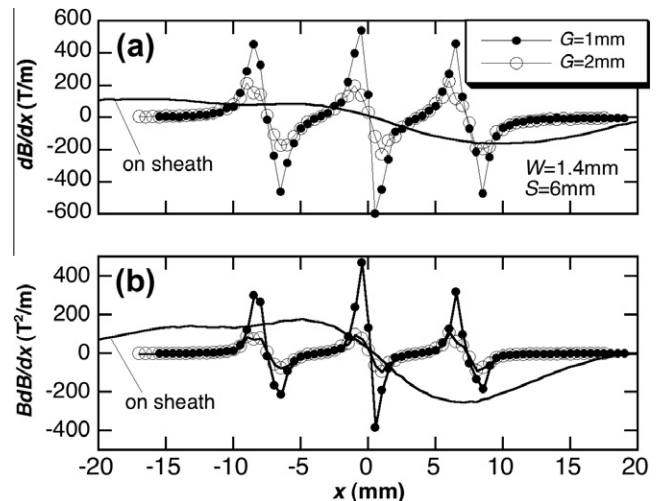


Fig. 7. Magnetic gradient dB/dx and the magnetic force coefficient BdB/dx profiles for the condition ($W = 1.4$ mm, $S = 6$ mm, $G = 1$ mm), for which ΔB was the largest in this study. The dB/dx and BdB/dx profiles for the condition ($W = 1.4$ mm, $S = 6$ mm, $G = 2$ mm) and those on the vacuum sheath are also shown.

In summary, we investigated the realization of the spatially modulated magnetic field using two-aligned superconducting bulk magnets and silicon steel bundles. Two bulks were magnetized along opposite direction by pulsed fields and were magnetically coupled with three pairs of the silicon steel bundles with a narrow open gap. We studied systematically the spatially magnetic field modulation ΔB and the magnetic force coefficient BdB/dx , as functions of the thickness of the bundles (W), the space between the bundles (S), and the open gap width (G). As a result, $\Delta B = 0.76$ T and $BdB/dx = 500$ T²/m were realized in the open gap. We plan to apply the spatially magnetic modulation to the solution growth of organic semiconductors.

Acknowledgement

This work was partially supported by Japan Science and Technology Agency under a Research for Promoting Technological Seeds 2008 (02–035).

References

- [1] B. Crone, A. Dodabalapur, Y.-Y. Lin, R.W. Filas, Z. Bao, A. LaDuca, R. Sarpeshkar, H.E. Katz, W. Li, *Nature* 403 (2000) 521.
- [2] M. Halik, H. Klauk, U. Zschieschang, G. Schmid, C. Dehm, M. Schltz, S. Maisch, F. Effenberger, M. Brunnbauer, F. Stellacci, *Nature* 431 (2004) 963.
- [3] A.R. Murphy, J.M.J. Frechet, *Chem. Rev.* 107 (2007) 1066.
- [4] M. Ito, W.Y. Li, N. Yoshimoto, H. Muraoka, S. Ogawa, H. Fujishiro, Y. Asabe, J. Ackermann, C. Videlot-Ackermann, H. Brisset, F. Fages, *Mol. Cryst. Liq. Cryst.* 491 (2008) 264.
- [5] N. Hirota, T. Homma, H. Sugawara, K. Kitazawa, M. Iwasaki, S. Ueno, H. Yokoi, Y. Kakudate, S. Fujiwara, M. Kawamura, *Jpn. J. Appl. Phys.* 34 (1995) L991.
- [6] N. Yoshimoto, unpublished.
- [7] T. Uemura, M. Sugitani, M. Kumakura, T. Kimura, *J. Photopol. Sci. Technol.* 20 (2007) 113.
- [8] H. Fujishiro, A. Fujiwara, T. Tateiwa, T. Oka, H. Hayashi, *IEEE Trans. Appl. Supercond.* 16 (2006) 1080.